Heritage Science

RESEARCH

Open Access

The Warring States period faience beads excavated from Majiayuan Cemetery: characterization and new insights

Liu Liu[1†], Yaozheng Zheng[2†], Yuchen Tang[1], Shiqi Cai[3], Yan Xie[4], Junchang Yang[2,3] and Zhanyun Zhu[3,5*]

Abstract

In 2006, the Majiayuan Cemetery of the Warring States period (475 BCE to 221 BCE) was discovered in Zhangjiachuan county of Gansu province, northwest China. The thousands of exquisite gold/silver artifacts, bronze wares, potteries, and beads unearthed, and have attracted great interest when investigating the dynamics of exchange, mobility, and transcultural encounters in Eurasian artifacts. During the excavation, plenty of blue and purple faience beads were found arranged around the tomb owner in grave M52. Faience beads of the same style unearthed from other graves of the region indicate their mature production at the time of burials. By adopting scientific methods for the chemical and compositional characterization of the faience beads, this study explained their materials and production techniques and provided new insights into faience production in the late Warring States period.

Keywords Faience beads, Han purple, Han blue, The Warring States period

Introduction

First appearing in the Near East and Egypt toward the end of the 5th century BCE, faience is thought to have spread to Europe [1, 2] and suddenly appeared in the Central Plains of China with the rise of the Western Zhou Dynasty (1046 BCE to 771 BCE), about 3000 years later compared with the western countries [3, 4]. New excavations in Xinjiang (northwestern China) provided further information regarding early faience in China during the middle 2nd millennium BCE, which resulted from the exchange of artifacts [5, 6]. The faience production in China was developed during the Han Dynasty (202 BCE to 220 CE). Faience artifacts were mainly shaped as beads and occasionally vessels. Together with other beads/metal, the faience beads were used in ornament for decoration or symbols of status and wealth [7]. Plenty of Western Zhou Dynasty faience artifacts shaped as round, tubular, and rhombic beads have been excavated along the Yellow River and the Yangtze River. The earliest natron glasses found in China are eye beads excavated from high-status burials from the late Spring and Autumn period to the early Warring States period [8]. Characterizing the flux could provide important evidence regarding the provenance of the faience beads, based on the different types of faience, such as soda-rich, mixed alkali, and potash-rich faience. Faience artifacts with high sodium and mixed alkali were found to be the earliest faience in China [9]. With the development of technology, glass production thrived and gradually replaced the faience production

†Liu Liu and Yaozheng Zheng contributed equally to this work.

*Correspondence:
Zhanyun Zhu
zhanyun.zhu@xmu.edu.cn; zhu@shh.mpg.de
[1] Xiamen Academy of Arts and Design, Fuzhou University, Xiamen 361000, China
[2] School of Materials Science and Engineering/Institute of Culture and Heritage, Northwestern Polytechnical University, Xi'an 710072, China
[3] Conservation Science Laboratory/Department of Archaeology, Joint Research Center for Revolutionary Cultural Relics, School of History and Cultural Heritage, Xiamen University, Xiamen 361005, China
[4] Gansu Provincial Institute of Cultural Relics and Archaeology, Lanzhou 730015, China
[5] Department of Archaeology, Max Planck Institute of Geoanthropology, 07745 Jena, Germany

during the Warring States period. The adoption of lead and barium as flux in glass/faience production was found exclusively in China since the same period [10, 11].

Technical characterization of faience beads worldwide has been reported in various case studies, focusing on the recognition of the bead structures, chemical composition and flux identification, to better understand the craft and provenance of the faience [9, 10, 12–16]. Studies on colorants have attracted great interests among the questions that have been posed. Blue and purple were highly regarded as noble colors due to their rarity. Thus, ancient civilizations invented blue and purple pigments, such as Egyptian Blue, Han Blue (HB), and Han Purple (HP) [17]. Egyptian blue is considered the first synthetic pigment, with quite high stability [18–20]. Egyptian blue has been used as a colorant or pigment since around 3600 BCE and has been widely used in Greece and the Roman Empire. In China, local synthetic pigments HB and HP appeared gradually. HB and HP were accidentally obtained as byproducts from the research on superconductors in the 1980s and later identified on painted ancient objects and in octagonal sticks artificially prepared by ancient Chinese craftsman [21, 22]. The application of HB and HP dates back to the Western Zhou period (1046 BCE to 771 BCE) and lasted for the subsequent centuries [23]. Studies on beads excavated from different graves in the Majiayuan Cemetery have been reported, including the identification of HB and HP as colorants, and the characterization of their elementary composition [23–25]. With the benefit of the access to the newly unearthed beads during excavation, the research team performed a close observation and raised the question that whether the beads were different from the reported ones. By conducting the following research, the raised question could be illuminated, and new insights would be shared at both regional and inter-regional levels.

Archeological context

Located in Zhangjiachuan county of Gansu province, northwest China, the Majiayuan Cemetery (Fig. 1) was discovered in 2006. Over 80 graves of the late Warring States period with abundant burial objects were discovered, and the excavation continued for the following 16 years. Thousands of exquisite gold/silver artifacts, bronze wares, pottery, and beads were unearthed. Centered in the cemetery, tomb M6 is surrounded by smaller tombs and sacrificial pits of different sizes. Its owner is believed to be one of the highest-level local elites, according to the unearthed artifacts. It's quite noteworthy that chariots decorated with gold/silver/iron foils and beads were found in 75% of the tombs, some of which were lacquered with black/red and green patterns. Various ornaments and decorations were unearthed, including earrings, necklaces, headwear, hat decorations, and belts, composed of different beads and metal accessories. The materials for the beads included faience, turquoise, red chalcedony, gold, and silver [26, 27]. The unearthed artifacts indicate the nobility of their owners, and provide great value for investigating the dynamics of exchange, mobility and transcultural encounters in Eurasian antiquity [28].

A completely degraded 'wooden coffin' was discovered in grave M52 of the Majiayuan Cemetery in 2015 with traces of its outline and several faience beads on its surface identified during excavation. The whole coffin was packed and relocated to the lab at Northwestern Polytechnical University, and the excavation proceeded under controlled temperature and humidity. With the help of scientific analyses alongside the excavation, the

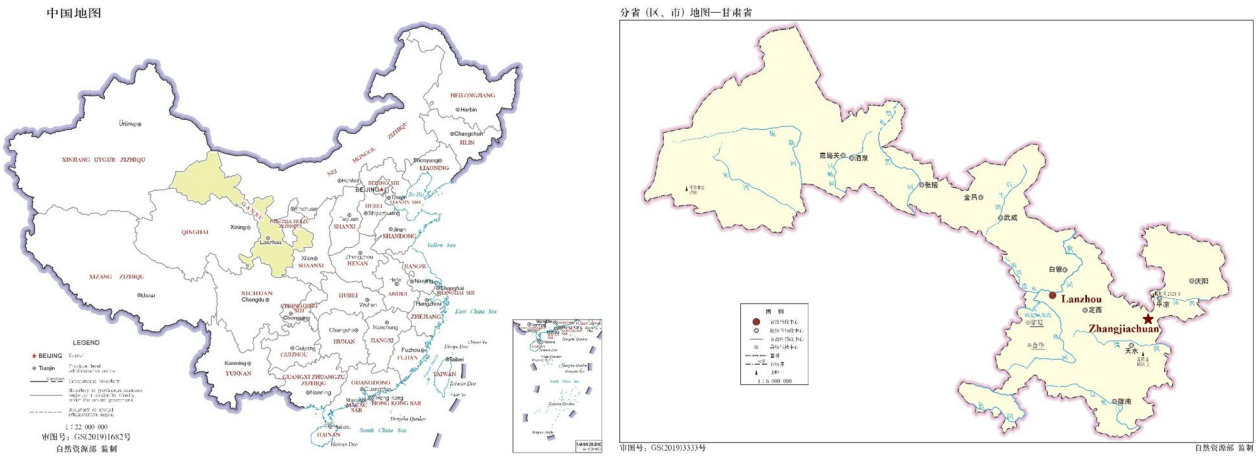

Fig. 1 Location of Majiayuan Cemetery in Zhangjiachuan county of Gansu province, China

burial artifacts can be clearly recongnized, which benefits a full-scale recording. Eventually, over 100 pieces of gold/silver artifacts used as trappings were unearthed. Plenty of faience beads were arranged around the owner of the tomb. Instead of a limited number of tubular beads and eye beads, thousands of plain blue and purple faience beads were discovered. Stacks of the unearthed faience beads were in poor condition with few in certain arrangements upon excavation.

Materials and methods

Materials

Plenty of purple and blue faience beads were arranged around the tomb owner's head, legs, and feet, most severely degraded and incomplete. The purple and blue faience beads were in regular shape and nearly the same size. As shown in Fig. 2, 16 beads (fragments) from different zones with the full structure were carefully selected under a microscope. The information of the collected samples is presented in Table 1. Some of the beads are blue, and the others are blue and purple. Some beads have white superficial deposits on their surface and inner layer. The beads are 1.4 to1.7 mm in internal diameter, 2.4 to 2.8 mm in external diameter, and 0.9 to 1.1 mm in height. Although tiny, the size of the beads is consistent, indicating a skillful production. Most beads have centered and straight perforations without drilling marks, and some perforations are filled with soil in burial condition. The beads are of poor strength and can break into pieces easily. Different scientific methods were applied to analyze each sample and understand the material and craft. In addition, 6 incomplete beads were selected and embedded (18-1, 30-1, 30-2, 52-1, 239-2, 240-2) to observe the layered structure and compositional characteristics. The undamaged beads were chosen for nondestructive analysis. Raman spectrometry was adopted to reveal the minerals and compounds. To minimize the destructive analysis, only fragments of sample 28 were collected for XRD analysis.

Methods

Microscopic analysis

The samples were observed under an Axio Scope A1 polarized microscope equipped with an ICCS optical system (Zeiss Ltd., Germany) and a VK-X250 three-dimensional digital microscope (Keyence Corporation, Japan) at magnification levels of 50 to 200 times and 20 to 200 times, respectively.

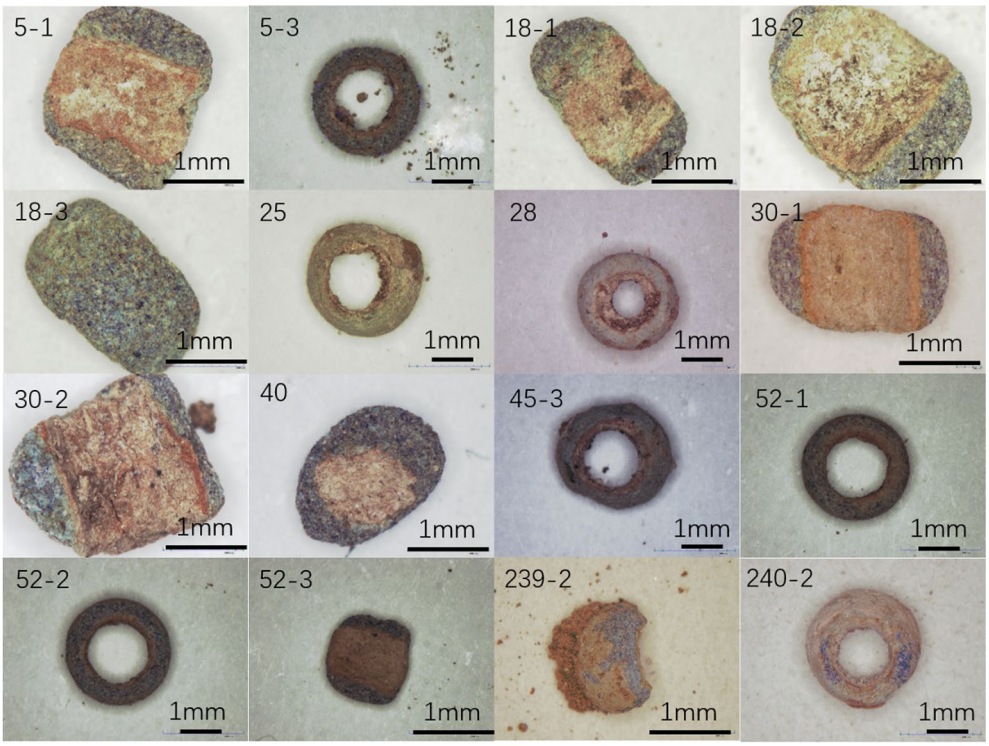

Fig. 2 The collected purple and blue faience beads

Table 1 Information of the collected samples

Sample no.	Description	Excavated Location	Method
5-1	Incomplete, blue and purple bead	Tomb owner's feet	OM, Micro-Raman spectroscopy
5-3	Blue and purple bead with full structure	Tomb owner's feet	OM, Micro-Raman spectroscopy
18-1	Incomplete, blue and purple bead, white superficial deposit on the surface	Tomb owner's left leg	OM, Micro-Raman spectroscopy, SEM-EDS
18-2	Incomplete, blue and purple bead	Tomb owner's left leg	OM
18-3	Incomplete, blue and purple bead	Tomb owner's left leg	OM
25	Blue and purple bead with full structure	Tomb owner's feet	OM, Micro-Raman spectroscopy
28	Blue and purple bead with full structure	Tomb owner's feet	OM, Micro-Raman spectroscopy, XRD
30-1	Incomplete, blue and purple bead	Tomb owner's left leg	OM, Micro-Raman spectroscopy, SEM-EDS, EPMA
30-2	Incomplete, blue and purple bead	Tomb owner's left leg	OM, SEM-EDS
40	Incomplete, blue bead	Tomb owner's head	OM, Micro-Raman spectroscopy
45-3	Blue and purple bead with full structure	Tomb owner's feet	OM
52-1	Blue and purple bead with full structure	Tomb owner's head	OM, SEM-EDS, EPMA
52-2	Blue and purple bead with full structure	Tomb owner's head	OM
52-3	Incomplete, blue and purple bead	Tomb owner's head	OM
239-2	Incomplete, blue and purple bead	Tomb owner's shoulder	OM, SEM-EDS
240-2	Incomplete, blue and purple bead	Tomb owner's right leg	OM, SEM-EDS

SEM-EDS (scanning electron microscopy in combination with energy dispersive X-ray analysis)

6 incomplete beads with full layer were selected, embedded by an inlaying machine (CitoVac, Struers Ltd., Denmark), and ground by a Tegramin-20 automatic grinding equipment (Struers Ltd., Denmark) to reach the surface of the samples. SEM-EDS analysis was conducted with a FEI Verios 4G SEM coupled with an Oxford X-max 20 EDS analyzer to obtain backscattered electron (BSE) images for phase and layered structure investigation. Samples were analyzed with a 20 kV acceleration voltage and 6.0 to 7.0 mm working distance. The samples were sputter coated with gold for the enhancing of conductivity prior to the test. Element characterization of each mineral/ area was achieved via EDS. The test at each spot/area was repeating for at least three times to eliminate the error caused by inhomogeneous. To test the composition of each layer, a relatively homogeneous area covering as much as possible was selected as the test zone, thus ensuring data accuracy and representativeness.

EPMA (electron probe microanalysis)

A Shimadzu EPMA-8050G was used for a more accurate elemental mapping of the surface of a blue and a purple bead, which was pre-treated with gold sputter coating to improve the conductivity. Five elements, i.e., O, Si, Cu, Ba, and Pb, were adopted for elemental mapping under the voltage of 15 kV.

Micro-Raman spectroscopy

A Renishaw inVia RM200 Raman spectrometer coupled with a microscope was used to characterize the minerals and compounds of the samples. Measurements were performed using an argon gas laser at 532 nm with a range 100 to 4000 cm $^{-1}$. Different color zones, such as light blue, blue, purple, white, and red layer were selected. The detection temperature was 25 °C, and the humidity was below 50%. The spectral resolution was 0.5 to 1 cm $^{-1}$, and the laser power was approximately 0.5 mW, thus ensuring good quality spectra. Samples were placed directly under the microscope to select interesting areas (colorants, white superficial deposit, and red layer) for detection. OriginPro 8.5 was used for spectra treatment.

XRD (X-ray diffraction)

To supplement the Micro-Raman spectroscopy, fragments of sample 28 were collected and ground into powder for XRD analysis using an X'Pert Pro MPD diffractometer (Philips, Netherlands) with a Cu-Ka radiation source ($\lambda = 0.15418$ nm) in the range of 5 to 95°, a tube voltage of 40 kV, and a current of 200 mA at a scan rate of 10°min^{-1}. Samples were ground into powder for analysis. XRD spectra was analyzed and matched by JADE.

Results and discussion

Microscopic structure

Microscopic analyses reveal a smooth and thin red layer (70 to 240 μm) with a clear boundary as the inner layer of

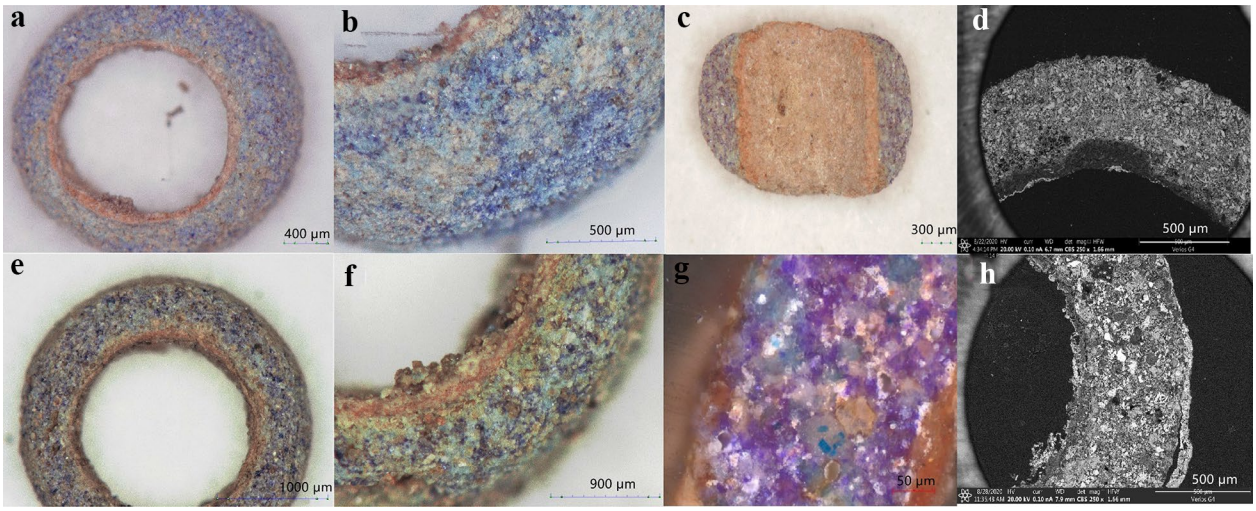

Fig. 3 Microscopic image of the beads. **a** Surface of sample 28, **b** surface of sample 28, **c** inner layer of sample 30-1, **d** surface of 30-1 by SEM, **e** surface of sample 52-1, **f** surface of sample 52-1, **g** surface of 52-2 by polarized microscope, **h** surface of 240-2 by SEM

the beads (Fig. 3a, b, e, f). The red layer was also reported in beads excavated from other tombs of the Majiayuan Cemetery [24]. The perforation of the beads is straight, without traces of carving or drilling (Fig. 3c), demonstrating the beads were made with the "core forming" technique, namely, using certain materials as the inner core of the beads before modeling, and removing the core after heating. Unlike faience beads excavated from Shanxi and Tibet [29, 30], the rim of each faience bead in M52 stayed intact without the sign of shearing, indicating that the beads were made separately one by one before heating. The material used as the inner core remain unclear. If the red layer was the residue of the inner core, the traces resulting from removing the core were not found. According to a previous study [31], mineral and organic materials (e.g., wood) were selected to simulate the inner core. After the beads were made, the mineral core firmly bonded with the beads' body and became impossible to remove, while the organic core was easily removed. In this case, we assume the organic materials were used as the inner core and disappeared after heating, leaving a smooth interface. The formation of the red layer might be attributed to a different inhomogeneous heating pathway since it was next to the inner core, or it was simply caused by the use of iron rich soil as the mineral material for the core forming technique.

The colorants for the blue faience beads include both light blue and dark blue particles (Fig. 3a and b), while those for the blue and purple faience beads include both light blue and purple particles, with blue particles easily found in such samples (Fig. 3e, f, g). Xia et al. pointed out that HB and HP were frequently found together in the same sample, indicating that they were produced together. HB is more stable than HP [32]. According to previous research, some of the Majiayuan faience beads had a glaze layer, and the colorants of the purple beads could be attributed to HP alone or the combination of HP, HB, and Han dark blue ($BaCu_2Si_2O_7$) [23–25]. Fading (weathering degradation) could be observed on the surface of the faience with white superficial deposits (Figs. 2 and 3b, f). The colorants were flaking off inhomogeneously on both categories of faience beads.

Two different layered structures were identified. Most of the beads show no clearly defined boundaries for identifying the classic triple-layered structure of faience objects, as shown in Fig. 3d. However, two of the embedded beads exhibit 25 to 60 μm surface layers with clear boundaries loosely connectied with the bead's body, resulting in peeling off (Figs. 3h and 4d).

SEM-EDS/EPMA analysis

The SEM-EDS results and EPMA mapping are presented in Figs. 4 and 5; Table 2. SEM examinations of the beads exhibit a heterogeneous structure with different minerals. As exemplified by samples 30 − 2 and 52 − 1 (Fig. 4), the beads were porous, with the surface layer partially visible. Continuous interparticle glass or interaction layer were not formed due to the heating temperature and crafts. The concentration of Pb was detected on the surface layer, outer edge, and inner edge (Figs. 4a and 5) with isolated Pb particles found on the body of the bead (Fig. 4c). Ba was not identified from the surface layer but was distributed randomly in the bead's body. Different minerals can be observed in Fig. 4e, micro analysis of each region by EDS is shown in Table 2 51-1-1 to 51-1-4. Noteworthy,

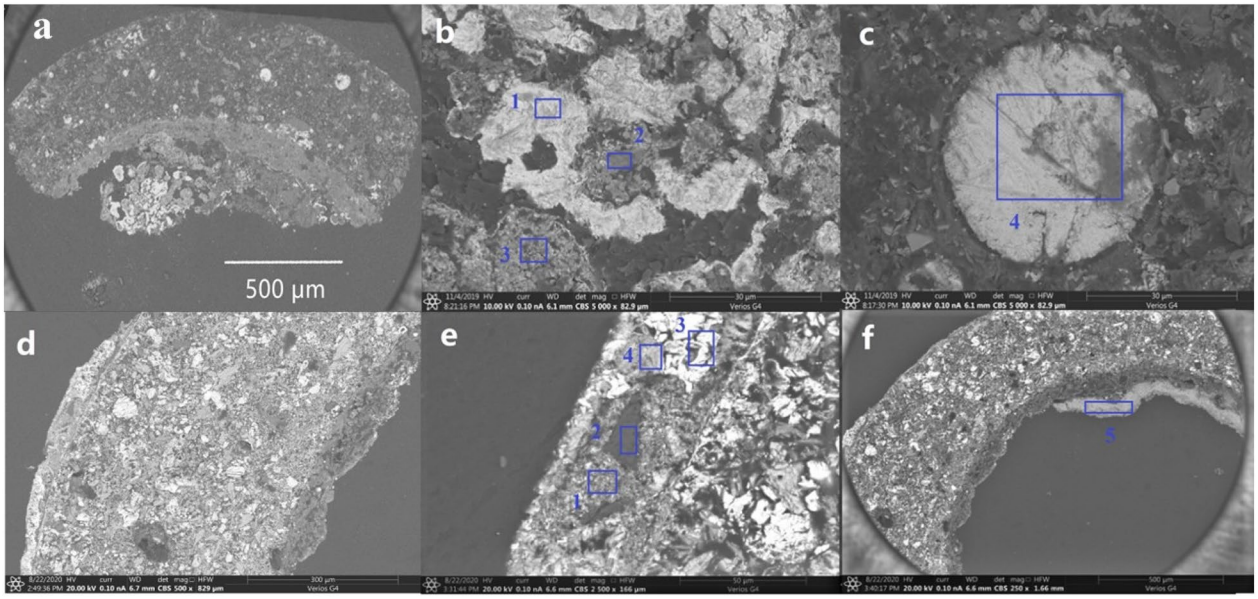

Fig. 4 SEM-EDS analysis of the beads. **a**–**c** Surface and tested areas of sample 30-2, **d**–**f** surface and tested areas of sample 52-1

Table 2 Results of SEM-EDS analysis of the samples concentrations are given as weight% (wt%) in oxide form

Sample no.	Na_2O	MgO	Al_2O_3	SiO_2	SO_3	K_2O	CaO	Fe_2O_3	CuO	BaO	PbO
18-1 body	–	–	1.05	33.95	5.52	–	–	0.85	12.65	33.66	12.32
18-1 red layer	4.64	2.50	11.83	54.26	–	4.15	3.93	6.42	4.20	3.84	4.23
30-1 body	–	–	0.75	33.95	5.72	–	–	–	12.03	35.88	11.67
30-1 red layer	3.45	3.32	9.77	64.23	–	2.21	3.74	10.72	2.56	–	–
30-2 body	–	–	0.52	30.44	–	–	–	–	12.78	32.76	23.50
30-2 red layer	3.23	2.66	12.67	54.48	–	2.82	4.64	12.15	4.89	–	2.46
30-2-1	–	–	–	–	–	–	–	–	7.59	29.20	63.20
30-2-2	–	10.94	12.26	24.04	–	3.73	–	16.95	7.21	4.39	20.49
30-2-3	–	–	–	–	–	–	–	–	20.4	–	79.6
30-2-4	–	–	5.08	–	–	–	–	–	–	–	94.92
52-1 body	–	–	0.47	35.90	6.94	–	–	0.75	12.24	33.65	10.05
52-1 red layer	4.37	1.93	11.32	52.11	–	2.14	3.37	8.24	4.85	7.48	4.19
52-surface layer	–	–	2.57	4.02	–	–	10.59	–	7.63	–	75.20
52-1-1	–	–	1.67	3.98	–	1.04	9.73	–	7.33	–	76.25
52-1-2	–	–	–	96.03	–	–	–	–	3.96	–	–
52-1-3	–	–	1.41	–	–	–	3.27	–	6.57	–	88.76
52-1-4	–	–	–	–	–	–	9.74	–	6.37	–	83.89
52-1-5	–	–	0.33	2.28	–	–	0.43	94.39	2.57	–	–
239-2 body	0.74	–	0.65	33.77	–	0.25	0.10	–	11.93	35.4	17.25
239-2 red layer	5.02	2.16	10.84	56.31	2.26	2.53	3.50	5.97	3.84	7.57	–
240-2 body	–	–	2.10	35.95	0.80	–	1.15	–	27.45	25.90	6.65
240-2 red layer	3.67	2.03	14.42	56.13	–	2.04	3.67	7.08	–	9.92	1.04

some studies pointed out a misunderstanding of the quartz-free glaze layer (GLZ) and interaction layer (IAL) in Chinese faience. The glaze layer has peeled off in most Chinese faience due to its glazing method and weathering degradation [33]. The surface layer might be IAL instead of GLZ since the quartz particle in the GLZ layer has melted to the glass state, and SiO_2 would not appear as crystals [4, 5, 34]. According to Fig. 4e,

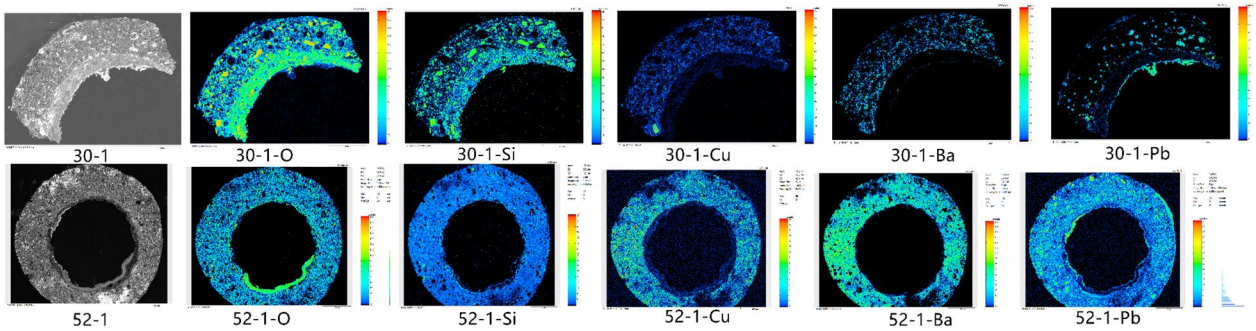

Fig. 5 EPMA-mapping of different elements of the bead 30-1 and 52-1

the SiO_2 in the surface layer stayed as crystal with side lengths of 15.21 μm, 26.91 μm, and 35.10 μm. Three faience bead glazing method have been found, i.e., the efflorescence method, direct application, and cementation method. The efflorescence method has frequently been applied to glassy faience, where the body and glaze layer are thoroughly mixed and highly glassified. For the faience beads in this study, the body was not highly glassified, and seldom surface layer was observed. Despite the great significance of revealing their forming and glazing methods separately, the glazing method of the studied faience beads remains unclear due to the limited evidence.

The two possible sources of quartz used in the faience beads production can be distinguished based on the particles shape: angular ones been crushed quartz pebbles and normally rounded ones being sand particles. Crushed quartz pebbles have high purity [19], while the sand grain morphology dependents on the sand maturity degrees, with immature sands having mainly angular and subangular grains. Angular quartz particles are distributed inhomogeneously among the tested beads (Fig. 4d) with high purity of up to 96 wt% (Table 2 51-1-2). Besides, it is important to note that the quartz studied in this part might come from IAL, likely partially fused. Some particles may appear rounded, and there may have been minor incorporation of other elements. It has been proved that copper can in fact be incorporated into the structure of heated quartz but in trace amounts [35]. In this case, the source of the quartz still needs further discussion.

Different kinds of minerals, such as quartz, lead carbonate, and minerals with Al and K were identified from the surface layer (Fig. 4e). The body of the beads consists of colorants, quartz, Pb particles, and feldspar (Fig. 4b and c). Na was identified in the red layer (inner layer) but not detected in the body and surface layer. Additionally, the Fe content in the red layer was significantly higher than in the bead body. The different elements indicate that the red layer might have different mineral sources than the bead body or originate from the residue of the inner core. Meanwhile, Fe and O are concentrated next to the red layer (Figs. 4f and 5 HP-O), and the reason remained unclear.

S was detected in the samples, which might be ascribed to $BaSO_4$, one possible raw material of HB and HP. A ternary diagram of SiO_2*-CuO*-BaO* is shown in Fig. 6, where the data are normalized by Si, Cu, and Ba. In summary, the tested data clustering together, showing a stable ingredient of the beads with a higher content of Ba compared with the theoretical value (especially for HP).

Micro-Raman spectroscopy /XRD analysis

The colorants and other minerals are identified through micro-Raman spectroscopy (Fig. 7; Table 3) and XRD (Fig. 8). Areas with different colors were selected under a microscope before Micro-Raman spectroscopy analysis. HB phase and SiO_2 were identified from the blue and light blue areas with minor traces of HP in samples

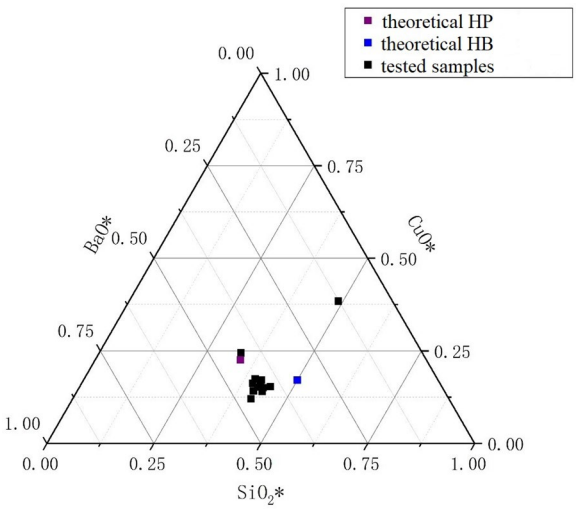

Fig. 6 Ternary diagram of SiO*-CuO*-BaO* of the tested faience beads

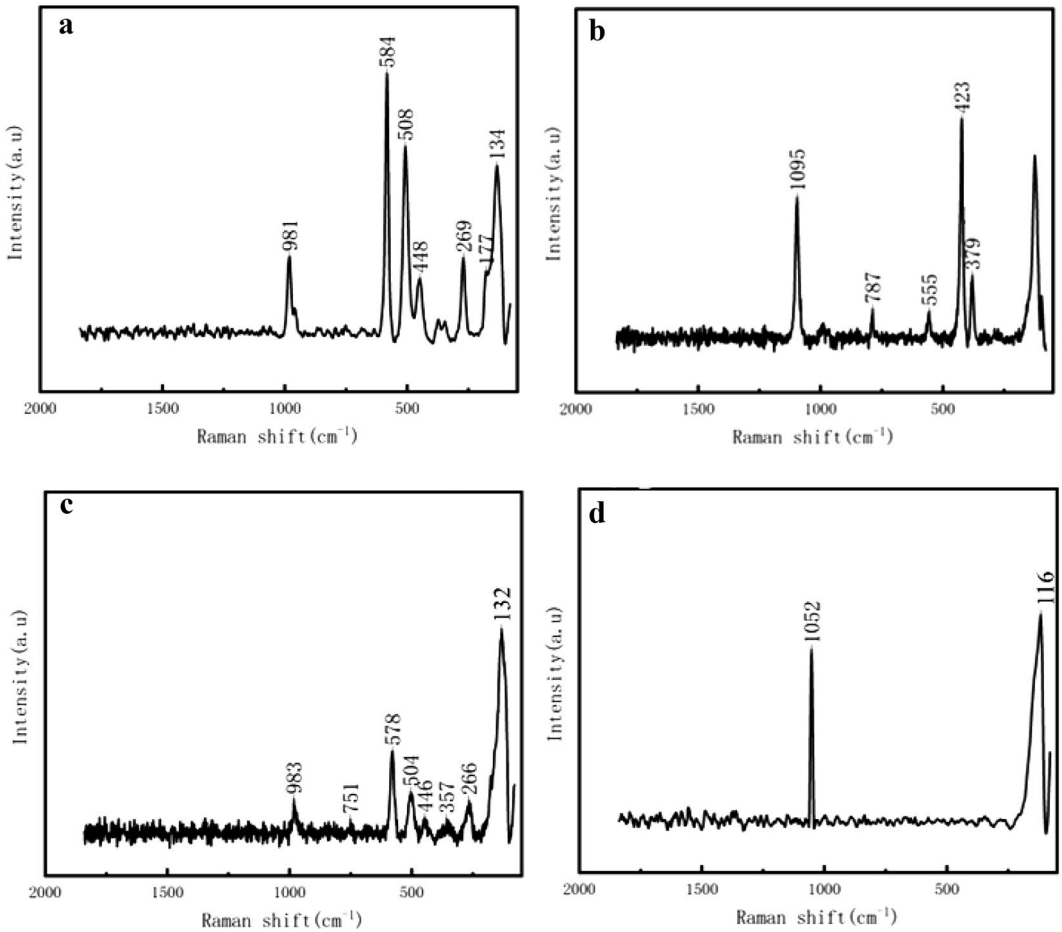

Fig. 7 Micro-Raman spectra of **a** light blue area of sample 5-3 **b** blue area of sample 30-1, **c** purple area of sample 25 **d** white area of sample 25

Table 3 Micro-Raman spectra of the tested areas (cm^{-1})

5-1 blue	5-3 light blue	18-1 blue	30-1 blue	40 blue	Phase or functional group	25 purple	28 purple	40 purple	Phase or functional group
1095	–	–	1095	1086	HB	983	985	986	HP/$BaSO_4$
–	981	985	987	–	HB	751	–	–	$Si_3O_9^{6-}$
–	–	–	787	–	HB	578	588	581	HP/δ(SiO_2)
–	584	587	555	–	HB	504	516	505	HP/$Si_4O_{12}^{8-}$
–	508	516	–	–	Si_4O_{12}	446	466	449	HP/SiO_2
–	448	464	–	–	SiO_2	–	382	374	HP/(CuO)
423	–	–	423	423	SiO_3^{2-}(glass)/HB	357	356	–	HP
379	370	–	379	379	HB	–	274	–	HP/(CuO)
–	346	355	–	–	HP	266	–	269	β-$BaSi_2O_5$
–	269	275	–	273	β-$BaSi_2O_5$	–	240	–	HP

5-3 and 18-1. For HB, the characteristic band around 1102 cm^{-1} is assigned to a_{1g} ν(SiO) vibration, while the band around 427 cm^{-1} is attributed to a_{1g} bridging oxygen breathing modes [36]. Previous research has shown the presence of HP based on Raman spectra, with characteristic bands around 985, 587, 516, 464, 355, and 273 cm^{-1} [37–39]. Bands of β-$BaSi_2O_5$ were found with very strong bands in the range of 967 to 961 cm^{-1}, indicating

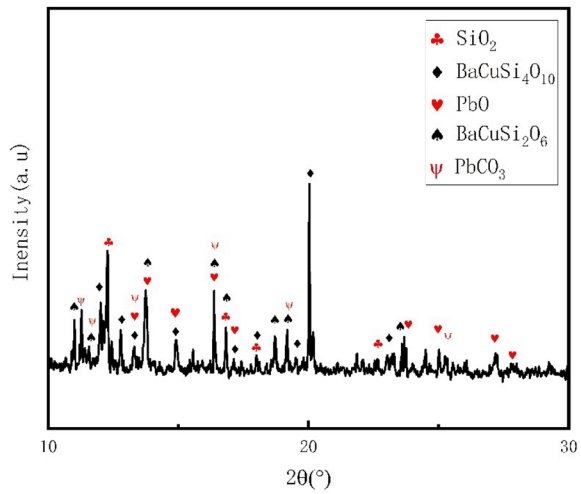

Fig. 8 XRD of the sample 28

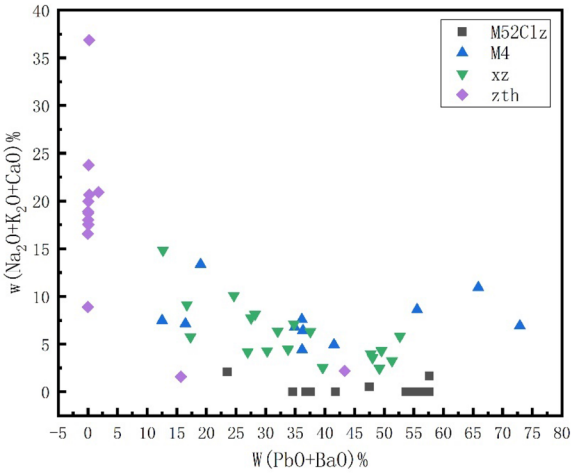

Fig. 9 The componential comparison of faience. (M52Clz: faience tested in this paper, M4: grave M4 from Majiayuan cemetery [25], xz: Xin Zheng [47], zth: Zhaitouhe [48])

the presence of orthosilicates (SiO_4^{4-}) [40]. In this study, however, only the band around 268 cm^{-1} was identified in the blue and purple areas, which could be attributed to β-$BaSi_2O_5$. In the simulated HP preparation, $BaSi_2O_5$ was detected when $BaCO_3$ was adopted as the Ba source, which was assumed to be an intermediate product [41].

The white superficial deposits on the beads were analyzed. The band at 1052 cm^{-1} (Fig. 7d) is the characteristic band of $PbCO_3$ formed during the weathering of Pb-Ba glass by the chemical reaction among Pb, CO_2, and water vapor, resulting in the gradual accumulation of $PbCO_3$ on the surface of the glass [42]. Since the decomposition temperature of $PbCO_3$ is much lower than the bead glazing temperature, the $PbCO_3$ in the samples is generated during the weathering of the beads.

Apart from the previously identified minerals, PbO is detected via XRD (Fig. 8). According to the simulated synthesis of HB and HP, minerals with Pb were added as flux and the catalyst to lower the decomposition temperature of $BaSO_4$ or $BaCO_3$, which is crucial to the synthesis of HP with poor thermostability [41, 43]. Unfortunately, Micro-Raman spectroscopy and XRD spectra of the red layer showed no significant bands of minerals with Fe.

Raw materials of HB and HP

As early synthetic pigments/colorants, the raw materials of HB and HP have been discussed extensively. Simulation experiments were conducted to verify the hypotheses [36, 44]. $BaSO_4$ and $BaCO_3$ were tried as the Ba source for the synthesis of HP. Unlike the previously reported study of the beads from Majiayuan Cemetery [24, 45], $BaSO_4$ was detected by micro-Raman spectroscopy in M21, while areas with S and Ba in the ratio of 1:1 were discovered in some faience beads. In this study, seldom S was detected, and $BaSO_4$ was not detected by Micro-Raman spectroscopy or XRD characterization. A previous study pointed out that barium copper silicate minerals and HP could be easily produced with $BaCO_3$ as the Ba source material [46]. β-$BaSi_2O_5$ was identified by Micro-Raman spectroscopy as the intermediate product during HP synthesis with $BaCO_3$ as the raw material [41]. In conclusion, the Ba source of faience beads in grave M52 might originate from $BaCO_3$.

Faience production in the Warring States period

As the local silicate system in China, the Pb-Ba rich faience/glass was widely discovered among the Chu State in the Warring States period with obviously regional characteristics. There is a growing consensus among the craftsman of bronze ware production at the early stage that adding a certain amount of Pb decreases the melting temperature and increases the fluidity of the raw materials. Thus, Pb was adopted as the flux of glass/faience production in succession. The componential comparison of Pb-Ba rich faience unearthed in different sites of the Warring States period is shown in Fig. 9. The archaeological sites are located along the Yellow River Basin, from the Central Plains to northwest China. Two different componential systems (i.e. soda-rich faience and Pb-Ba rich faience) were found in the Zhaitouhe Cemetery. Unlike other tested samples, faience in M52 has a constant low concentration of Na_2O-K_2O-CaO and a lower fluctuation of PbO-BaO. Nevertheless, the PbO-BaO content of faience beads has a relatively concentrated range instead of a random recipe. Apart from the plain faience beads, the tested samples in M4 of the Majiayuan Cemetery include

different tubular and eye beads, possibly leading to the compositional variation that could be explained by the study of similar beads in M52. It would also be interesting to see whether the composition of faience beads is relevant to the rank of the grave in the same cemetery.

Conclusions

This study scientifically analyzed the late Warring States period faience beads excavated from grave M52, Majiayuan cemetery, and demonstrated the diversity of materials and techniques of Pb-Ba rich faience production. The findings are of great significance to gaining new insights, and tracing such artifacts produced at the end of faience production and the beginning of the glass industry. This study revealed that the beads were produced using the "core forming" technique. The severe weathering, leading to the partially visible glaze layer and concentrated Pb on the edge of rims. Moreover, it's quite interesting to find the Fe-rich mineral next to the inner rim of a HP bead. HB and HP were identified as colorants, and the Ba source was assumed to have originated from $BaCO_3$. The ratio of Pb-Ba-Si was kept within a specific range for stable HP and HB production.

Abbreviations

HB	Han blue
HP	Han Purple
OM	Optical microscope
SEM-EDS	Scanning electron microscopy in combination with energy dispersive X-ray analysis
XRD	X-ray diffraction

Acknowledgements

The authors are extremely grateful to Gansu Provincial Cultural Heritage Administration, Prof. Guoke Chen, Prof. Tianzhen Deng from Gansu Provincial Institute of Cultural Relics and Archaeology, Prof. Hui Wang from Fudan University, Prof. Congcang Zhao from Northwest University, Prof. Xiaojuan Dang from Shaanxi Institute for the Preservation of Cultural Heritage, Prof. Nicole Boivin, Ms. Kristin Starkloff, Ms. Anja Schatz from Max Planck Institute of Geoanthropology, Mr. Huabin Xie from Xiamen University Archive, Ms. Ying Huang from School of History and Cultural Heritage—Xiamen University, and Dr. Guoliang Li from Xiamen Academy of Arts and Design—Fuzhou University for their help in providing access to the samples, supervision of archaeological excavation and research, as well as technical support in scientific analysis and administration.

Author contributions

The manuscript was written through the contributions of all authors. All authors have given approval to the final version of the manuscript.

Funding

Open Access funding enabled and organized by Projekt DEAL. This work is supported by China Ministry of Education Humanities and Social Sciences Project (19YJCZH105), China Scholarship Council (202206655001), and The Alexander von Humboldt Foundation.

Availability of data and materials

All data generated or analyzed during this study are included in this published article.

Declarations

Competing interests

The authors declare no competing interests.

Received: 21 March 2023 Accepted: 16 September 2023
Published online: 10 October 2023

References

1. Purowski T. New data on the technology of faience production in central Europe in the early bronze age. Archaeometry. 2020;62(3):563. https://doi.org/10.1111/arcm.12543.
2. Tite MS, Maniatis Y, Kavoussanaki D, Panagiotaki M, Shortland AJ, Kirk SF. Colour in Minoan faience. J Archaeol Sci. 2009;36(2):370–8. https://doi.org/10.1016/j.jas.2008.09.031.
3. Hommel P, Sax M. Shifting materials: variability, homogeneity and change in the beaded ornaments of the western Zhou. Antiquity. 2014;88:1213–28. https://doi.org/10.1017/S0003598X00115418.
4. Lin Y, Rehren T, Wang H, Ren X, Ma J. The beginning of faience in China: a review and new evidence. J Archaeol Sci. 2019;105:97–115. https://doi.org/10.1016/j.jas.2019.03.007.
5. Wang Y, Rehren T, Tan Y, Cong D, Jia PW, Henderson J, et al. New evidence for the transcontinental spread of early faience. J Archaeol Sci. 2020;116:105093. https://doi.org/10.1016/j.jas.2020.105093.
6. Yang Y. Archaeometry should be based on archaeology. A comment on Lin et al. 2019. J Archaeol Sci. 2020;119:105149.
7. Gu Z, Zhu J, Xie Y, Xiao T, Yang Y, Wang C. Nondestructive analysis of faience beads from the western Zhou Dynasty, excavated from Peng State cemetery, Shanxi Province. China J Anal at Spectrom. 2014;8:1438–43. https://doi.org/10.1039/C4JA00031E.
8. Henderson J, An J, Ma H. The archaeometry and archaeology of ancient Chinese glass: a review. Archaeometry. 2018;60(1):88–104. https://doi.org/10.1111/arcm.12368.
9. Wen R, Hu X, Cao S, Wang Y. The dissemination of chinese potash-rich faience: investigation of faience beads from the Wupu cemetery, Xinjiang. Herit Sci. 2023;11(1):69. https://doi.org/10.1186/s40494-023-00901-y.
10. Wang Y, Ma H, Chen K, Huang X. Identification of PbO (BaO) faience from an early and middle Warring States period cemetery at Zhaitouhe, northern Shaanxi China. Archaeometry. 2019;1:43–54. https://doi.org/10.1111/arcm.12401.
11. Li Q, Dong J, Gan F. Discussion on chemical composition and craft of faience and glass production in early China. J Guangxi Minzu Univ. 2009;4:31–41.
12. Li Q, Gan F, Gu D. Questions of research of ancient Chinese glass. Stud Hist Nat Sci. 2007;2:234–47.
13. Liu N, Yan Y, Wang Y, Hu W, Jiang X, Ren M, et al. Nondestructive characterization of ancient faience beads unearthed from Ya'er cemetery in Xinjiang, early iron age China. Ceram Int. 2017;13:10460–7. https://doi.org/10.1016/j.ceramint.2017.05.086.
14. Dardeniz G, Yıldırım T, Yıldırım C, Çiftçi E. Techniques of Blue, Green, and White Faience Bead production used at the early bronze Age Central Anatolian Site of RESULOĞLU (Turkey). Archaeometry. 2021;63(2):327–42. https://doi.org/10.1111/arcm.12606.
15. Costa M, Barrulas P, Arruda AM, Barbosa R, Vandenabeele P, Mirão J. New approaches for the study of faience using beads from Southern Portugal. J Archaeol Sci Rep. 2022;46: 103703. https://doi.org/10.1016/j.jasrep.2022.103703.
16. Napolitano MF, Blair EH, Dussubieux L, Fitzpatrick SM. Chemical analysis of glass beads in Palau, western Micronesia reveals 19th century inter-island exchange systems in transition. J Archaeol Science: Rep. 2022;45:103542. https://doi.org/10.1016/j.jasrep.2022.103542.
17. Berke H. Chemistry in ancient times: the development of blue and purple pigments. Angew Chem Int Ed. 2002;41(14):2483–7. https://doi.org/10.1002/1521-3773(20020715)41:14<2483::AID-ANIE2483>3.0.CO;2-U
18. García-Fernández P, Moreno M, Aramburu JA. Origin of the anomalous color of Egyptian and Han Blue historical pigments: going beyond the

complex approximation in ligand field theory. J Chem Educ. 2016;1:111–7. https://doi.org/10.1021/acs.jchemed.5b00288.
19. Hatton GD, Shortland AJ, Tite MS. The production technology of Egyptian blue and green frits from second millennium BC Egypt and Mesopotamia. J Archaeol Sci. 2008;61:591–604. https://doi.org/10.1016/j.jas.2007.11.008.
20. Grifa C, Cavassa L, De Bonis A, Germinario C, Guarino V, Izzo F, et al. Beyond vitruvius: new insight in the technology of Egyptian blue and green frits. J Am Ceram Soc. 2016;10:3467–75. https://doi.org/10.1111/jace.14370.
21. FitzHugh EW, Zycherman LA. A purple barium copper silicate pigment from early China. Stud Conserv. 1992;37(3):145–54. https://doi.org/10.1179/sic.1992.37.3.145.
22. FitzHugh EW, Zycherman LA. An early man-made blue pigment from China—barium copper silicate. Stud Conserv. 1983;28(1):15–23. https://doi.org/10.1179/sic.1983.28.1.15.
23. Berker H, Corbiere T, Potmann A, et al. Man-made ancient Chinese blue and purple pigments. Cult Relics. 2009;6:251–65.
24. Lin Y, Zhou G, Freestone I, Rehren T. Research on unearthed vitreous from the Warring States Cemetery in Zhangjiachuan, Majiayuan. Cult Relics. 2018;(3):71–83. https://doi.org/10.13619/j.cnki.cn11-1532/k.2018.03.007
25. Huang X, Yan J, Wang H. Study on faience beads excavated in the Warring Stataes Majiayuan cemetery in Gansu Province. Spectrosc Spectr Anal. 2015;10:2895–900.
26. Zhou G, Fang Z, Xie Y, Ma M. 2006 Excavation on the Majiayuan Cemetery of the Warring States Period of Zhangjiachuan Autonomous County of Hui Nationlity, Gansu. Cult Relics. 2008;(9):4–28.
27. Wang H. Treasures of Xiron. Press of Cultural Relics. 2014;10–31.
28. Liu Y, Xi T, Ma J, Liu R, Kuerban R, Yan F et al. Art historical and archaeometric analyses of the animal style gold and silver ornaments (4th-3rd century BCE) found in Northwest China. Archaeometry. https://doi.org/10.1111/arcm.12725.
29. Liu Y, Wang Y, Chen K, Mei J, Ma H, Li C, Zhu L, Xie Y. Analysis of unearthed faience beads from grave M6043 in Dahekou. Archaeol Cult Relics. 2019;2:114–9.
30. Cao S, Wen R, Yu C, Shargan W, Tash T, Wang D. New evidence of long-distance interaction across the Himalayas: Faience beads from western Tibet. J Cult Herit. 2021;47:270–6. https://doi.org/10.1016/j.culher.2020.09.010.
31. Gu Z. A study about the relationship between Chinese faience and early glass. The University of Chinese Academy of Science, Beijing; 2015.
32. Xia Y, Ma Q, Zhang Z, Liu Z, Feng J, Shao A, et al. Development of chinese barium copper silicate pigments during the Qin Empire based on Raman and polarized light microscopy studies. J Archaeol Sci. 2014;49:500–9. https://doi.org/10.1016/j.jas.2014.05.035.
33. Dong J. Restudy on the technical origin and development of ancient Chinese glass. Shanghai Institute of Optics and Fine Mechanics; 2020.
34. Lei Y, Xia Y. Study on production techniques and provenance of faience beads excavated in China. J Archaeol Sci. 2015;53:32–42. https://doi.org/10.1016/j.jas.2014.09.019.
35. Rottier B, Rezeau H, Casanova V, Kouzmanov K, Moritz R, Schlöglova K, et al. Trace element diffusion and incorporation in quartz during heating experiments. Contrib Miner Petrol. 2017;172(4):23. https://doi.org/10.1007/s00410-017-1350-4.
36. Bouherou S, Berke H, Wiedemann H-G. Ancient man-made copper silicate pigments studied by Raman Microscopy. Chimia. 2001;55(11):942–51. https://doi.org/10.2533/chimia.2001.942.
37. McKeown DA, Bell MI. Four-membered silicate rings: vibrational analysis of $BaCuSiO_6$ and implications for glass structure. Phys Rev B. 1997;56(6):3114–21. https://doi.org/10.1103/PhysRevB.56.3114.
38. Chen Y, Zhang Y, Feng S. Hydrothermal synthesis and properties of pigments chinese purple BaCuSi2O6 and dark blue BaCu2Si2O7. Dyes Pigm. 2014;105:167–73. https://doi.org/10.1016/j.dyepig.2014.01.017.
39. Cheng X, Xia Y, Mal Y, Lei Y. Three fabricated pigments (Han purple, indigo and emerald green) in ancient chinese artifacts studied by Raman microscopy, energy-dispersive X-ray spectrometry and polarized light microscopy. J Raman Spectrosc. 2008;38(10):1274–9. https://doi.org/10.1002/jrs.1766.
40. Ma Q, Portmann A, Wild F, Berke H. Raman and SEM studies of man-made barium copper silicate pigments in ancient Chinese artifacts. Stud Conserv. 2006;51(2):81–98. https://doi.org/10.1179/sic.2006.51.2.81.
41. Zhang Z, Ma Q, Mei J, Berke H. Simulative preparation of ancient Chinese silicion copper barium pigment. J Natl Mus China. 2012;(2):128–40.
42. Wu Z. Studies on microsopic morphology, micro-chemical compositio and weathering of ancient glass. J Chin Electron Microscopy Soc. 1984;(4):132.
43. Berke H, Wiedemann HG. The chemistry and fabrication of the anthropogenic pigments chinese blue and purple in ancient China. East Asian Sci Technol Med. 2000; (17): 94–120. https://www.jstor.org/stable/43150591.
44. Pabst A. Structures of some tetragonal sheet silicates. Acta Crystallogr A. 1959. https://doi.org/10.1107/S0365110X5900216X.
45. Li Q, Yang J, Li L, Dong J, Zha H, Liu S. Identification of the man-made barium copper silicate pigments among some ancient Chinese artifacts through spectroscopic analysis. Spectrochim Acta Part A Mol Biomol Spectrosc. 2015. https://doi.org/10.1016/j.saa.2014.11.060.
46. Qin Y, Wang YH, Chen X, Li HM, Li XL. A discussion on the emergence and development of ancient Chinese artificial barium copper silicate pigments from simulation experiments. Archaeometry. 2016. https://doi.org/10.1111/arcm.12205.
47. Fu Q, Zhao H, Dong J, Li Q, Hu Y. Nondestructive analysis of silica artefacts unearthed from Baofeng and Xinzheng in Henan Province. Spectrosc Spectr Anal. 2014;(1): 257–62.
48. Huang X, Wang L, Yan J, Sun Z, Sun Z, Li J. Studies on the enearthed silica decoration beads unearthed from Zhaitouhe, north Shaanxi. Archaeol Cult Relics. 2018;2:129–35.

Publisher's Note